

A Sampling-based Framework for Hypothesis Testing on Large Attributed Graphs [Scalable Data Science]

Yun Wang[†], Chrysanthi Kosyfaki[†], Sihem Amer-Yahia[§], Reynold Cheng[†]

[†]The University of Hong Kong, Hong Kong SAR, China

[§]CNRS, Univ. Grenoble Alpes, Grenoble, France

carrie07@connect.hku.hk;{kosyfaki,ckcheng}@cs.hku.hk;sihem.amer-yahia@univ-grenoble-alpes.fr

ABSTRACT

Hypothesis testing is a statistical method used to draw conclusions about populations from sample data, typically represented in tables. With the prevalence of graph representations in real-life applications, hypothesis testing in graphs is gaining importance. In this work, we formalize node, edge, and path hypotheses in attributed graphs. We develop a sampling-based hypothesis testing framework, which can accommodate existing hypothesis-agnostic graph sampling methods. To achieve accurate and efficient sampling, we then propose a Path-Hypothesis-Aware Sampler, PHASE, an m -dimensional random walk that accounts for the paths specified in a hypothesis. We further optimize its time efficiency and propose PHASE_{opt}. Experiments on real datasets demonstrate the ability of our framework to leverage common graph sampling methods for hypothesis testing, and the superiority of hypothesis-aware sampling in terms of accuracy and time efficiency.

1 INTRODUCTION

Hypothesis testing finds widespread application in various domains such as marketing, healthcare, and social science [21]. Hypotheses are usually tested on representative samples since it is impractical or even impossible to extract data from entire populations due to size, accessibility or cost. For instance, snowball sampling has been proven effective in accessing a hidden population like drug abusers through a chain-referral mechanism [11, 29]. In this paper, we study hypothesis testing on graphs.

Graphs can be used to represent many real-world applications such as social, bibliographic and transportation networks where entities are nodes and edges reflect relationships between entities. Specifically, we work on Attributed Graphs that are graphs with multiple types of nodes and edges, both of which are labeled with attributes containing valuable information for graph analytics [5, 22]. In a bibliographic network like DBLP (see Figure 1a and Figure 1b for an example and an attributed path of length one, respectively), hypotheses expressed on nodes, edges, and paths unveil interesting aspects of collaboration behavior and research trends based on citation evolution over time. Specifically, a node hypothesis can be “the average citation of conference papers is greater than average”, and a path hypothesis can be “the minimum number of citations of conference papers written by Microsoft researchers is greater than average”. Similarly, on social platforms like Yelp, hypothesis testing can be used to check how different users review a product and study its adoption.

Objectives and Challenges. Given an input attributed graph \mathcal{G} , our aim is to verify a hypothesis H and return true or false.

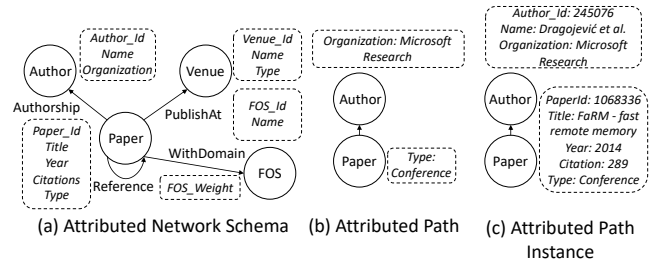


Figure 1: DBLP network schema and paths

We hence seek to achieve two objectives: **O1** - hypothesis testing should be as accurate as possible; **O2** - execution time should be as small as possible. To the best of our knowledge, there is no existing literature addressing hypotheses on attributed graphs. A straightforward approach is to obtain a sampled graph \mathcal{S} from \mathcal{G} using *hypothesis-agnostic* graph sampling methods [1, 18, 20]. However, the challenge is that depending on the sampling method and on the budget B , i.e., the size of \mathcal{S} , the **hypothesis estimator**, which computes aggregated values of nodes, edges, or paths specified in the hypothesis may return different values on \mathcal{S} and \mathcal{G} . This raises the accuracy challenge behind **O1**. Additionally, as B increases, the accuracy of the resulting hypotheses increases. However, the speed at which the accuracy converges highly depends on the sampling. This raises the efficiency challenge behind **O2**.

Contributions. We classify hypotheses on attributed graphs into three types: node, edge, and path hypotheses. We develop a sampling-based hypothesis testing framework, which accommodates common hypothesis-agnostic sampling methods, such as random node sampler [25], simple random walk [10], and non-backtracking random walk [16].

The lack of awareness of the input hypothesis in existing sampling methods may slow down the convergence speed of accuracy. Indeed, the sampled graph \mathcal{S} should preserve as many *relevant* paths according to H from \mathcal{G} as possible for a path hypothesis. Therefore, to address objectives **O1** and **O2**, we design PHASE, a Path-Hypothesis-Aware Sampler. PHASE *is aware of H* and preserves its nodes, edges, or paths. Consequently, the resulting \mathcal{S} is more likely to provide relevant information for testing the hypothesis. PHASE employs $m \geq 1$ dependent random walks with two weight functions to ensure path-hypothesis-awareness. One function biases the seed selection toward the first node in the path hypothesis. The other biases the transition probability towards the nodes specified in the hypothesis. We further propose PHASE_{opt} to improve the time efficiency of PHASE. PHASE_{opt} reduces computation overhead through random sampling of neighbors. It also

adopt a non-backtracking approach to prioritize the selection of relevant nodes, edges, and paths. We demonstrate both theoretically and empirically that the hypothesis estimator on \mathcal{S} converges to its corresponding value in \mathcal{G} as B increases.

We conduct extensive experiments on three real-world datasets: MovieLens, DBLP, and Yelp. We aim to demonstrate the effectiveness of the optimizations in PHASE_{opt} compared to PHASE, and to compare hypothesis-agnostic and hypothesis-aware samplers in terms of test significance, accuracy, and running time.

We first observe that PHASE_{opt} is at least 20 times faster than PHASE. Then, by comparing PHASE_{opt} with 11 state-of-the-art hypothesis-agnostic samplers, we find it achieves the best accuracy given the sampling budget across various hypothesis types and datasets. PHASE_{opt} also exhibits fast convergence of hypothesis estimators and robust accuracy performance especially for hypotheses with longer paths or limited relevant nodes, edges, or paths in \mathcal{G} . For significance, PHASE_{opt} consistently provides the most precise and reliable estimate, achieving the highest hypothesis significance among all samplers. Moreover, PHASE_{opt} achieves high accuracy in the shortest amount of time, making it usable in practice.

2 DEFINITIONS

2.1 Attributed Graphs

DEFINITION 1 (ATTRIBUTED GRAPH). *An attributed graph is a directed graph $\mathcal{G} = (\mathcal{V}, \mathcal{E})$, where \mathcal{V} denotes the set of nodes and $\mathcal{E} \subseteq \mathcal{V} \times \mathcal{V}$ is the set of edges, represented by ordered pairs of nodes. It has a node type mapping function $\phi : \mathcal{V} \rightarrow \mathcal{T}$ and an edge type mapping function $\psi : \mathcal{E} \rightarrow \mathcal{R}$. Each node and edge has attributes.*

Each node v in \mathcal{G} belongs to a specific node type $\phi(v) \in \mathcal{T}$, and each edge $e = (u, v)$ connecting nodes of type $\phi(u)$ to $\phi(v)$ belongs to a specific edge type $r = \psi(e) \in \mathcal{R}$. Once the relation r exists, its inverse relation r^{-1} naturally holds from $\phi(v)$ to $\phi(u)$. In this work, we assume each node in \mathcal{G} has at least one incoming or outgoing edge. It implies the connectedness of the graph.

The DBLP Network in Figure 1a is an attributed graph containing four types of nodes and four types of edges. For example, paper nodes belong to the node type `paper` $\in \mathcal{T}$ with five attributes, including title and year. The edge from `paper` to `field of study (FOS)` nodes is denoted by `WithDomain` $\in \mathcal{R}$, with a weight indicating the paper’s relevance to a particular FOS. The reverse relationship `WithDomain`⁻¹ $\in \mathcal{R}$ also holds from FOS to paper nodes.

DEFINITION 2 (PATH). *A path \mathcal{P} is defined as*

$$t_1 \xrightarrow{r_1} \dots \xrightarrow{r_l} t_{l+1}$$

where the node type t_i and edge type r_i can repeat; $l \geq 0$ is the length of \mathcal{P} . When $l = 0$, \mathcal{P} is a node and when $l = 1$, it is an edge.

An **attributed path** is a path where each node has a list of attributes, referred to as a **modifier**. Figure 1b presents an example of a length-one attributed path, “conference papers written by Microsoft researchers”, and Figure 1c is an instance of that path.

2.2 Hypotheses on Attributed Graphs

We formally define path hypotheses on attributed graphs. Node and edge hypotheses are two special cases of path hypotheses.

DEFINITION 3 (PATH HYPOTHESIS). *Given a path $\mathcal{P} = t_1 \xrightarrow{r_1} t_2 \xrightarrow{r_2} \dots \xrightarrow{r_l} t_{l+1}$ in \mathcal{G} , where $l \geq 1$, a path hypothesis is defined as:*

$$H_{path} : P_c^o (\text{agg}(f_{\mathcal{P}} | M_{t_i}, \forall t_i \text{ on } \mathcal{P}))$$

where $o \in \{=, <, >, \leq, \geq\}$; $c \in \mathbb{R}$ is a constant value; P_w^o is the predicate in the format: equal, unequal, greater, or less than a value; $f_{\mathcal{P}}$ is any function of node and/or edge attributes on \mathcal{P} ; $\text{agg}(f_{\mathcal{P}} | M_{t_i}, \forall t_i \text{ on } \mathcal{P})$ is an aggregation function applying on $f_{\mathcal{P}}$ of all paths with nodes satisfying the corresponding modifiers.

In the DBLP network defined previously, co-authorship can be represented as a path:

$$\mathcal{P} = \text{author} \xrightarrow{\text{Authorship}^{-1}} \text{paper} \xrightarrow{\text{Authorship}} \text{author}$$

“The average citation of papers co-authored by Microsoft researchers is greater than 100” can be expressed as:

$$P_{100}^> (\text{avg}(f_{\mathcal{P}} | \text{author}[\text{MSR}], \text{paper}[], \text{author}[\text{MSR}]))$$

where $f_{\mathcal{P}} = \text{paper}[\text{citation}]$, MSR stands for microsoft research.

When \mathcal{P} has length zero, a path hypothesis is reduced to a **node hypothesis**. An example of node hypothesis in the DBLP dataset can be “the average number of citations for conference papers is larger than 50” expressed as:

$$P_{50}^> (\text{avg}(\text{paper}[\text{citation}] | \text{paper}[\text{conference}])))$$

When \mathcal{P} has length one, we refer it as an **edge hypothesis**. For instance, the edge hypothesis “the average FOS_weight of conference papers on data mining is larger than 0.5” can be expressed as:

$$P_{0.5}^> (\text{avg}(\text{WithDomain}[\text{FOS_Weight}] | \text{paper}[\text{C}], \text{FOS}[\text{DM}]$$

C (resp. DM) stands for conference papers (resp. DM data mining).

2.3 Problem Statement and Challenges

Given an attributed graph \mathcal{G} , our aim is to verify a node, edge, or path hypothesis H and return true or false.

To address our problem, we formulate two objectives: **O1** the hypothesis testing should be as accurate as possible; **O2** the overall execution time should be as small as possible.

When testing a hypothesis such as “the average number of citations for conference papers is larger than 50”, a common approach includes collecting representative sample data and computing an aggregate value. In this case, the aggregate value corresponds to the average number of citations. However, directly collecting all relevant, i.e., satisfying the modifiers in the hypothesis, nodes, edges, or paths from \mathcal{G} and computing an aggregate value can be time-consuming. Therefore, we adopt the commonly used approach of sampling the graph \mathcal{G} into a smaller representative graph \mathcal{S} . This assumes a sampling budget B that reflects the maximum size of \mathcal{S} . For the sake of simplicity, unless stated otherwise, we assume sampling an edge or a node requires the same unitary cost 1.

A **hypothesis estimator** returns the aggregated value of nodes, edges, or paths in a hypothesis. The challenge of addressing **O1** is that depending on the sampling method and the budget B , the hypothesis estimator obtained from \mathcal{S} may differ from that of \mathcal{G} . We propose to first examine the applicability of existing sampling methods for graphs. Our observation is that the accuracy of those methods increases slowly as B increases, resulting in longer times

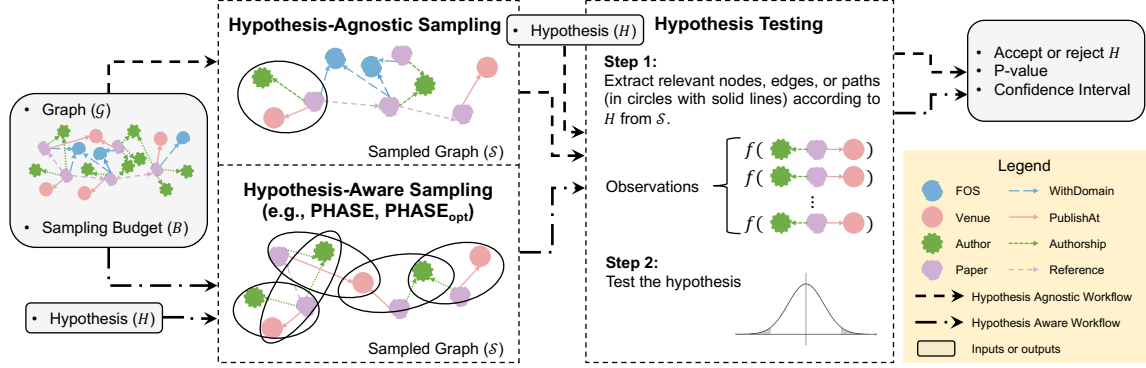


Figure 2: The Sampling-based Hypothesis Testing Framework on attributed graphs.

to achieve satisfactory accuracy. We conjecture that this is attributed to the lack of awareness of the underlying hypothesis during sampling. For instance, \mathcal{S} should preserve as many relevant paths from \mathcal{G} as possible for a path hypothesis. Hence, to address objective **O2**, we seek to design a sampling method that is *aware of H* and preserves relevant nodes, edges, or paths in H . We further aim to demonstrate both theoretically and empirically that using our sampling, the hypothesis estimator on resulting \mathcal{S} converges to its corresponding value in \mathcal{G} as B increases.

3 SAMPLING-BASED HYPOTHESIS TESTING

We propose a sampling-based hypothesis testing framework that supports both hypothesis-agnostic and hypothesis-aware graph samplers. After reviewing existing hypothesis-agnostic methods, we introduce our hypothesis-aware sampler, PHASE, in Section 3.2.1. It addresses objective **O1** by ensuring convergence of hypothesis estimators, and objective **O2** by incorporating hypothesis awareness into the sampling. Additionally, we implement two optimizations, PHASE_{opt}, to reduce the running time of PHASE in Section 3.2.2.

3.1 Hypothesis-Agnostic Samplers

Figure 2 illustrates the sampling-based hypothesis testing framework we propose to test node, edge, and path hypotheses on attributed graphs. Based on whether the graph sampling method is hypothesis-agnostic or hypothesis-aware, there are two workflows indicated by dashed and dash-dot-dash arrows, respectively. Their distinction lies in where the hypothesis H is introduced. In the hypothesis-aware workflow, H is necessary during the sampling step, while in the hypothesis-agnostic workflow, H is directly introduced before hypothesis testing.

Following dashed arrows from the left, the first procedure is to sample a graph \mathcal{S} using a hypothesis-agnostic sampler, which requires \mathcal{G} and B only. The existing hypothesis-agnostic samplers can be categorised into three categories: node samplers that choose B nodes from \mathcal{G} [1, 25], edge samplers that choose B edges from \mathcal{G} [15], and random walk based samplers that pick edges and nodes through the process of random walks [10, 16–18]. The second procedure is to conduct the hypothesis testing using \mathcal{S} and H . Specifically, we extract all relevant nodes, edges, or paths from \mathcal{S} and compute the required aggregated values for hypothesis testing. Finally, the

Algorithm 1 PHASE

Input: $\mathcal{G} = (\mathcal{V}, \mathcal{E})$, B , H
Output: a sampled graph \mathcal{S}

- 1: Initialize $L = (v_1, v_2, \dots, v_m)$ with m randomly chosen nodes
- 2: $L_w = \text{AssignWeight}(L, H)$ ▶ Assign w_h to x_1 nodes and w_l to other nodes.
- 3: $\mathcal{V}_S = \{\}, \mathcal{E}_S = \{\}$
- 4: **while** $B > m$ **do**
- 5: Normalize L_w
- 6: Select $v \in L$ with probability L_w
- 7: $N \leftarrow N[v]$ ▶ $N[v]$ is the set of neighbors of v .
- 8: $N_w = \text{AssignWeight}(N, H)$ ▶ Assign weights to nodes in N according to the transition probability matrices.
- 9: Select $u \in N$ with probability N_w
- 10: $\mathcal{V}_S.\text{update}(v, u)$
- 11: Replace v by u in L and update L_w
- 12: $B = B - 1$
- 13: **end while**
- 14: **return** $\mathcal{S} = \{\mathcal{V}_S, \mathcal{E}_S\}$

acceptance or rejection result, p-value, and confidence interval are returned.

3.2 Hypothesis-Aware Samplers

3.2.1 PHASE Algorithm. We introduce PHASE, our Path-Hypothesis-Aware Sampler (Algorithm 1). PHASE aims to preserve nodes, edges, or paths specified in a hypothesis H . It can be integrated with any random walk based sampler that maintains the path-preserving property. To ease understanding, we illustrate it with *FrontierS* [24]. *FrontierS* picks a node from m random seeds based on degree-proportional probability and performs a random walk by uniformly selecting a neighbor to proceed. It repeats the process until reaching the sampling budget B .

PHASE takes \mathcal{G} , B , and H as inputs. For a node, edge, or path hypothesis, H contains \mathcal{P} with lengths zero, one, or more than one, respectively. It initializes m seed nodes randomly in a list L (Line 1), which increases the probability of selecting relevant nodes, edges, and paths from \mathcal{G} . Each seed is assigned a weight in L_w (Line 2) to guide the selection of seed nodes for random walks later. These weights are determined based on heuristics, with nodes satisfying the first node modifier on \mathcal{P} (denoted by x_1) assigned a higher weight w_h and all other nodes assigned a lower weight w_l .

| | | | | | | | | | | | | |
|-------|-------|-------|-------|-------|-------|-------|------------|------------|-------|-------|-------|-------|
| | x_1 | y | | x_1 | x_2 | y | | x_1, x_1 | w_l | w_h | w_l | w_l |
| x_1 | w_h | w_l | x_1 | w_l | w_h | w_l | x_1, x_2 | w_l | w_l | w_h | w_l | |
| y | w_h | w_l | x_2 | w_h | w_l | w_l | x_1, x_3 | w_h | w_l | w_l | w_l | |
| | | | y | w_h | w_l | w_l | x_1, y | w_h | w_l | w_l | w_l | |
| | | | | | | | | | | | | |

(a)
(b)
(c)

Figure 3: Transition probability matrices for node (a), edge (b), and path ($l = 2$) (c) hypotheses, where $w_h \geq w_l > 0$ denote transition probabilities. x_i represents nodes in \mathcal{G} satisfying the i -th node modifier on \mathcal{P} , while y represents nodes not satisfying any node modifier on \mathcal{P} . (a) and (b) involve 1st-order random walks, whereas (c) involves 2nd-order random walks because the probability of selecting the next node depends on both the current and previous nodes.

Lines 4-14 describe an iterative random walk to select nodes until B is reached. During each iteration, the algorithm chooses a node v from L with probability L_w (Line 6). Then, it selects one of v 's neighbors u using a weighted selection process (Lines 7-9). Specifically, in Line 9, we adjust the transition probability to bias the random walks towards nodes, edges, or paths that satisfy \mathcal{P} in H . The transition probability matrices for node, edge, and path hypotheses are depicted in Figures 3a, 3b, and 3c, respectively.

After adding nodes u and v to \mathcal{V}_S (Line 10), the algorithm updates L by replacing v with u (Lines 11) and decreases the sampling budget by one (Lines 12). This iteration continues until $B > m$. The resulting sampled graph \mathcal{S} is the induced subgraph from \mathcal{V}_S .

3.2.2 PHASE_{opt} Algorithm. We further propose optimizations to reduce execution time. Algorithm 2 introduces two lines that replace line 7 in Algorithm 1. Firstly, in densely connected graphs, the computation of neighbor weights in step 8 of Algorithm 1 can be time-consuming due to the potentially large number of neighbors. To mitigate this, we randomly sample a subset of $\min\{|N|, n\}$ neighbors as candidates for selection, where n is a parameter. Secondly, we adopt a non-backtracking approach by avoiding the selection of visited nodes during the sampling process[16]. This strategy prevents cycles and unnecessary node visits.

Algorithm 2 PHASE_{opt}

(showing only 2 lines that replace line 7 in Algorithm 1)

-
- 1: $N' \leftarrow N[v] - \mathcal{V}_S$ (Optim 2)
 - 2: $N \leftarrow \text{Select min}\{|N'|, n\}$ nodes randomly from N' (Optim 1)
-

Complexity. On average, each node has $2|\mathcal{E}|/|\mathcal{V}|$ neighbors to be examined by PHASE, resulting in a time complexity of $O(B \times 2|\mathcal{E}|/|\mathcal{V}|)$. On the other hand, by constraining the number of neighbors, PHASE_{opt} achieves a time complexity of $O(B)$.

3.2.3 Convergence of Hypothesis Estimators. Let us demonstrate the convergence of hypothesis estimators using our proposed sampling algorithms (Challenge 1).

By Lemma 5.1 from[24], *FrontierS* is equivalent to the sampling process of a SRW over $\mathcal{G}^m = (\mathcal{V}^m, \mathcal{E}_m)$, where \mathcal{G}^m is the m -th Cartesian power of \mathcal{G} and

$$\mathcal{V}^m = \{(v_1, \dots, v_m) | v_1 \in \mathcal{V} \wedge \dots \wedge v_m \in \mathcal{V}\}$$

is the m -th Cartesian power of \mathcal{V} . $\forall \mathbf{u}, \mathbf{v} \in \mathcal{V}^m$, $(\mathbf{u}, \mathbf{v}) \in \mathcal{E}_m$ if there exists i such that $(u_i, v_i) \in \mathcal{E}$ and for all $j \neq i$, $u_j = v_j$. Given \mathcal{G} is a directed, connected, and non-bipartite graph, in the steady state, the sampled edges of *FrontierS* form a stationary sequence and satisfy the following Strong Law of Large Numbers (SLLN), the proof of which can be found in [24].

THEOREM 1 (SLLN). For any function f , where $\sum_{(u,v) \in \mathcal{E}} |f(u,v)| < \infty$,

$$\lim_{B \rightarrow \infty} \frac{1}{B} \sum_{i=1}^B f(u_i, v_i) \rightarrow \frac{1}{|\mathcal{E}|} \sum_{(u,v) \in \mathcal{E}} f(u,v)$$

almost surely, i.e. the event occurs with probability one.

For a path hypothesis with length l , it involves $(l - 1)$ -th order random walk, which is equivalent to a SRW over $\mathcal{G}^{l-1} = (\mathcal{V}^{l-1}, \mathcal{E}_{l-1})$ [19]. Hence, PHASE's random walks can be viewed as a SRW over $\mathcal{G}^{l-1+m} = (\mathcal{V}^{l-1+m}, \mathcal{E}_{l-1+m})$. As PHASE ensures that the resulting random walks over \mathcal{G}^{l-1+m} maintain both irreducibility and aperiodicity, it preserve stationarity and adhere to the SLLN. PHASE_{opt} also follows the SLLN because the stationary distribution of the NBRW remains the same as that of the SRW.

By Theorem1, we can construct hypothesis estimators for node, edge, and path hypotheses and prove their convergence. Here, we focus on scenarios where agg represents an average function. The hypothesis estimators for other aggregation functions, such as maximum and minimum, can be derived in a similar manner.

A path hypothesis ($l \geq 2$): $\text{avg}(f_{\mathcal{P}} | M_{t_i}, \forall t_i \text{ on } \mathcal{P})$ has a primary subject $f_{\mathcal{P}}$. Let \mathcal{P}^* be all relevant paths in \mathcal{G} , and $\mathcal{P}_{\mathcal{G}}$ be all paths with the same length as \mathcal{P} in \mathcal{G} . The mean value of the path hypothesis, θ_{path} , is

$$\theta_{path} = \frac{1}{|\mathcal{P}^*|} \sum_{\mathcal{P} \in \mathcal{P}_{\mathcal{G}}} T(\mathcal{P}) \quad (1)$$

where $T(\mathcal{P}) = f_{\mathcal{P}} \times \mathbb{1}_{M_{t_i} \subseteq \mathcal{L}_{\phi(t_i)} \forall t_i \text{ on } \mathcal{P}}$. Replacing \mathcal{G} with the sampled graph \mathcal{S} , the estimator for θ_{path} is

$$\hat{\theta}_{path} = \frac{1}{|\mathcal{P}^* \cap \mathcal{P}_{\mathcal{S}}|} \sum_{\mathcal{P} \in \mathcal{P}_{\mathcal{S}}} T(\mathcal{P}) \quad (2)$$

When B goes to infinity, \mathcal{S} converges to \mathcal{G} . By Theorem1, we have

$$\lim_{B \rightarrow \infty} \frac{1}{|\mathcal{P}^* \cap \mathcal{P}_{\mathcal{S}}|} \sum_{\mathcal{P} \in \mathcal{P}_{\mathcal{S}}} T(\mathcal{P}) \rightarrow \frac{1}{|\mathcal{P}^*|} \sum_{\mathcal{P} \in \mathcal{P}_{\mathcal{G}}} T(\mathcal{P}) \quad (3)$$

almost surely. Hence, $\hat{\theta}_{path}$ is an asymptotically unbiased estimator of θ_{path} . Hypothesis estimators for node and edge hypotheses can be derived similarly.

4 EXPERIMENTS

The goal of our experiments is twofold: 1) test the effectiveness of optimizations in PHASE_{opt} compared to PHASE (Section 4.3), and 2) compare hypothesis-agnostic and hypothesis-aware samplers in

Table 1: Statistics of datasets

| Dataset | #(Nodes) | #(Edges) | Density | #(Node Types) | #(Edge Types) |
|-----------|-----------|------------|----------|---------------|---------------|
| MovieLens | 9,705 | 996,656 | 1.06e-02 | 2 | 1 |
| DBLP | 1,623,013 | 11,040,170 | 4.19e-06 | 4 | 4 |
| Yelp | 2,136,118 | 6,743,879 | 1.48e-06 | 2 | 1 |

terms of test significance (Section 4.4), accuracy (Section 4.5), and time (Section 4.6). The source code is publicly available ¹.

4.1 Experimental Setup

Datasets. We used three datasets [12, 27], extracted from real attributed networks: MovieLens, DBLP, and Yelp. Table 1 shows the statistics of the datasets.

Samplers We compare PHASE_{opt} with eleven existing samplers:

- Node samplers: Random Node Sampler (*RNS*), Degree-Based Sampler (*DBS*)
- Edge samplers: Random Edge Sampler (*RES*)
- Random walk based samplers: Simple Random Walk (*SRW*), Frontier Sampler (*FrontierS*), Non-Backtracking Random Walk (*NBRW*), Random Walk with Restarter (*RWR*), Metropolis-Hastings Random Walk (*MHRW*), Snow Ball Sampler (*SBS*), Forest Fire Sampler (*FFS*), Shortest Path Sampler (*ShortestPathS*)

Hypotheses. For each dataset (DB) and hypothesis type (N for node hypotheses), we provide three example hypotheses (labeled as DB-N1) in experiments. For example, on Yelp, we explore an edge hypothesis testing if “fast food average ratings exceed 4”. In DBLP, we examine a path hypothesis to see if “papers co-authored by Chinese institutes on data mining have over 50 citations”. To assess path length effects, we further test two path hypotheses with lengths of three and four in DBLP.

Parameter Choice. For PHASE and PHASE_{opt}, We set $m = 50$ to maintain the path-preserving capability of multi-dimensional random walks, and $n = 30$ to strike a balance between accuracy and time efficiency. Additionally, we choose $w_h = 10$ and $w_l = 0.1$ to regulate the bias towards relevant nodes, edges, and paths. The sampling budget B is maintained as a proportion of the total number of nodes in \mathcal{G} for all samplers. As for existing hypothesis-agnostic samplers, we use the best parameters in their respective settings. We report an average of 30 runs for every evaluation measure.

4.2 Evaluation Measures

Accuracy. Accuracy at a specific sampling proportion reflects the effectiveness of a sampling method. The accuracy below measures the number of matched hypothesis testing results on \mathcal{G} and \mathcal{S} :

$$\text{Accuracy} = \frac{1}{k} \sum_k \mathbb{1}_{H(\mathcal{G})=H(\mathcal{S})}$$

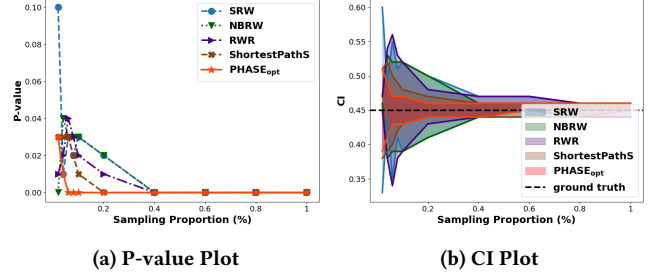
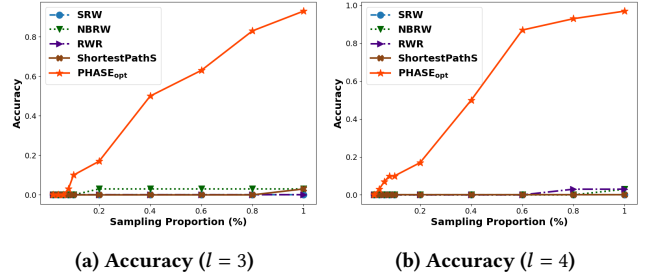
where $H(\mathcal{G})$ and $H(\mathcal{S})$ return 0 (false) or 1 (true).

Time. We measure the total execution time, including both the sampling time and the time taken to extract relevant information from \mathcal{S} for hypothesis testing.

¹<https://github.com/Carrieww/GraphHT>

Table 2: Average execution time (sec) of PHASE and PHASE_{opt} for DBLP node, edge, and path hypotheses.

| | Node | Edge | Path |
|----------------------|--------|--------|-------|
| PHASE | 115.66 | 539.15 | 441.3 |
| PHASE _{opt} | 5.56 | 8.76 | 5.91 |


Figure 4: DBLP p-value and CI plot for the hypothesis DB-P1

Figure 5: Accuracy versus sampling proportion plots for DBLP path hypotheses with length three (a) and four (b).

4.3 PHASE vs PHASE_{opt}

We evaluate the effectiveness of optimizations in PHASE_{opt} compared to PHASE using the DBLP dataset, as shown in Table 2. PHASE_{opt} is at least 20 times faster than PHASE while maintaining comparable accuracy (less than 5% accuracy reduction). Consequently, we exclusively use PHASE_{opt} for subsequent experiments.

4.4 Significance

To examine statistical significance and estimation precision, we analyze the trend of p-values and confidence intervals (CI) with increasing B . We illustrate this trend using a path hypothesis on DBLP as all other hypotheses show similar trends. As shown in Figure 4a, the p-value of PHASE_{opt} consistently stays below the significance level (e.g., 0.05) and decreases gradually. This trend indicates stronger evidence against the null hypothesis, showing higher statistical significance as B increases.

Figure 4b shows narrowing CI with increasing B , indicating more precise and reliable estimations of the hypothesis estimator. PHASE_{opt} consistently achieves the narrowest bound at any B , indicating the most precise and reliable estimate among all samplers.

4.5 Accuracy

Table 3 presents the accuracy performance of eleven existing samplers and PHASE_{opt} at a specific sampling proportion, shown in

Table 3: The accuracy of eleven existing samplers and PHASE_{opt} on three datasets and three types of hypothesis.

| Dataset | Hypothesis Type | Sampling Proportion (%) | PHASE _{opt} | RES | RNS | DBS | SRW | NBRW | RWR | MHRW | ShortestPathS | FrontierS | FFS | SBS |
|-----------|-----------------|-------------------------|----------------------|------|------|------|------|----------|------|------|---------------|-----------|------|------|
| MovieLens | Node | 1 | 0.9 | 0.89 | 0.83 | 0.86 | 0.88 | 0.89 | 0.87 | 0.89 | 0.86 | 0.84 | 0.83 | 0.56 |
| | Edge | 2.5 | 0.98 | 0.68 | 0.77 | 0.98 | 0.99 | 1 | 0.99 | 0.98 | 0.99 | 0.73 | 0.93 | 0.91 |
| | Path | 5 | 0.99 | 0.1 | 0.88 | 0.83 | 0.82 | 0.89 | 0.91 | 0.98 | 0.95 | 0.38 | 0.85 | 0.62 |
| DBLP | Node | 0.2 | 0.96 | 0.48 | 0.87 | 0.93 | 0.92 | 0.91 | 0.9 | 0.94 | 0.92 | 0.92 | 0.94 | 0.88 |
| | Edge | 0.2 | 0.76 | 0.48 | 0 | 0.71 | 0.73 | 0.69 | 0.7 | 0.29 | 0.69 | 0.63 | 0.7 | 0.42 |
| | Path | 0.2 | 0.89 | 0 | 0 | 0 | 0.26 | 0.3 | 0.32 | 0.18 | 0.33 | 0.043 | 0.3 | 0.12 |
| Yelp | Node | 0.1 | 0.99 | 0.65 | 0.77 | 0.61 | 0.69 | 0.69 | 0.69 | 0.77 | 0.7 | 0.64 | 0.66 | 0.48 |
| | Edge | 1 | 1 | 0.73 | 0.54 | 0.76 | 0.79 | 0.91 | 0.87 | 0.84 | 0.76 | 0.77 | 0.79 | 0.71 |
| | Path | 1 | 0.99 | 0.11 | 0.05 | 0.79 | 0.78 | 0.78 | 0.72 | 0.8 | 0.99 | 0.42 | 0.67 | 0.42 |

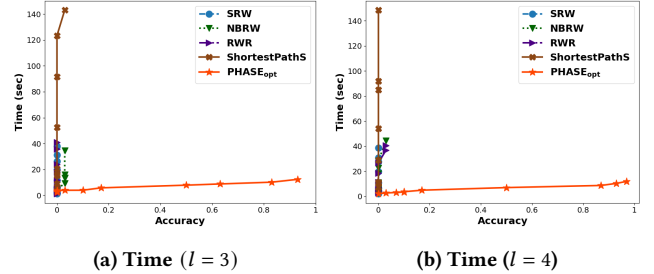
Table 4: The execution time (sec) of eleven existing samplers and PHASE_{opt} on three datasets and three types of hypothesis.

| Dataset | Hypothesis Type | Sampling Proportion (%) | PHASE _{opt} | RES | RNS | DBS | SRW | NBRW | RWR | MHRWS | ShortestPathS | FrontierS | FFS | SBS |
|-----------|-----------------|-------------------------|----------------------|-------|--------------|-------|-------|-------------|-------|-------|---------------|-----------|-------|-------|
| MovieLens | Node | 1 | 0.083 | 0.99 | 0.023 | 0.077 | 0.057 | 0.06 | 0.05 | 0.06 | 0.063 | 0.083 | 0.067 | 0.047 |
| | Edge | 2.5 | 0.45 | 0.99 | 0.11 | 0.36 | 0.31 | 0.36 | 0.33 | 0.29 | 0.26 | 0.33 | 0.35 | 0.31 |
| | Path | 5 | 4.92 | 1.03 | 0.34 | 4.32 | 4.53 | 4.55 | 4.76 | 3.10 | 0.95 | 0.38 | 3.87 | 3.08 |
| DBLP | Node | 0.2 | 5.56 | 18.70 | 0.55 | 6.98 | 7.98 | 8.22 | 9.67 | 1.66 | 31.32 | 10.48 | 5.73 | 3.03 |
| | Edge | 0.2 | 8.76 | 22.57 | 0.90 | 10.07 | 14.76 | 12.89 | 12.32 | 3.53 | 33.91 | 14.46 | 8.87 | 5.27 |
| | Path | 0.2 | 5.44 | 19.61 | 0.71 | 6.87 | 8.24 | 8.39 | 8.13 | 2.17 | 31.13 | 9.37 | 5.33 | 3.01 |
| Yelp | Node | 0.1 | 2.56 | 13.84 | 1.02 | 6.81 | 1.19 | 0.96 | 1.16 | 1.12 | 1.84 | 1.68 | 1.02 | 6.58 |
| | Edge | 1 | 19.42 | 16.88 | 2.01 | 13.61 | 8.58 | 8.97 | 9.17 | 6.93 | 30.23 | 10.22 | 10.27 | 6.03 |
| | Path | 1 | 56.97 | 14.35 | 1.53 | 23.48 | 15.97 | 16.61 | 19.03 | 7.35 | 37.81 | 9.95 | 25.61 | 19.94 |

column three. We select this proportion to balance stability and discriminative power, ensuring the accuracy is sufficiently stabilized without saturating across all samplers. For each dataset and type of hypothesis, the accuracy is the average accuracy of three hypothesis examples, each derived from an average of 30 runs. The highest accuracy in each row is highlighted in bold.

In Table 3, PHASE_{opt} demonstrates robust performance in all cases, except for MovieLens edge hypotheses, in where PHASE_{opt} slightly trails behind NBRW. Comparing among columns, some random walk based samplers, namely SRW, RWR, and ShortestPathS, exhibit good accuracy performance for edge and path hypothesis. On the contrary, RES, RNS, and DBS show ineffectiveness in handling path hypotheses. These observations align with their sampling mechanisms. These node and edge samplers can hardly preserve the path information from \mathcal{G} in the sampled graph. Additionally, comparing PHASE_{opt} and FrontierS, PHASE_{opt}'s superior performance indicates the efficacy of the two weight functions in enhancing the sampler's hypothesis-awareness to sample relevant nodes, edges, and paths.

We establish an accuracy ranking for all samplers by averaging their accuracy performance per column in Table 3 and select the top five: PHASE_{opt}, NBRW, ShortestPathS, RWR, and SRW. These samplers' accuracy convergence on individual hypotheses is compared in Figures 7 and 8 for DBLP and Yelp datasets, respectively. The figure for MovieLens is excluded due to space constraints and the similarity of results. In these figures, a-c, e-g, and i-k display the accuracy performance of three node, three edge, and three path hypotheses, respectively. Hypotheses of the same type are structured to have progressively fewer relevant nodes, edges, or paths in \mathcal{G} . The x-axis is truncated to clearly show the convergence.

**Figure 6: Time versus accuracy plots for DBLP path hypotheses with length three (a) and four (b).**

In Figures 7 and 8, PHASE_{opt} consistently outperforms other methods across all sampling proportions for most hypotheses. For hypotheses of the same type, PHASE_{opt}, with hypothesis-awareness, consistently demonstrates robust accuracy performance for the hypotheses with fewer relevant nodes, edges, or paths in \mathcal{G} . This is particularly evident for DBLP edge and path hypotheses. When relevant nodes, edges, and paths in \mathcal{G} are abundant, conventional sampling methods may have sampled a sufficient number of relevant nodes, edges, or paths to achieve high accuracy, which can diminish the distinctive advantage of PHASE_{opt}.

Delving into Figure 7, PHASE_{opt} dominates in node and path hypotheses for the DBLP dataset. However, ShortestPathS slightly outperforms PHASE_{opt} in edge hypotheses one and two, possibly due to the high betweenness centrality of these edges, implying that many shortest paths traverse those edges. Moving to Figure 8, PHASE_{opt} demonstrates clear superiority across all types of hypotheses for the Yelp dataset. Nonetheless, ShortestPathS occasionally exhibits competitive performance compared to PHASE_{opt} in

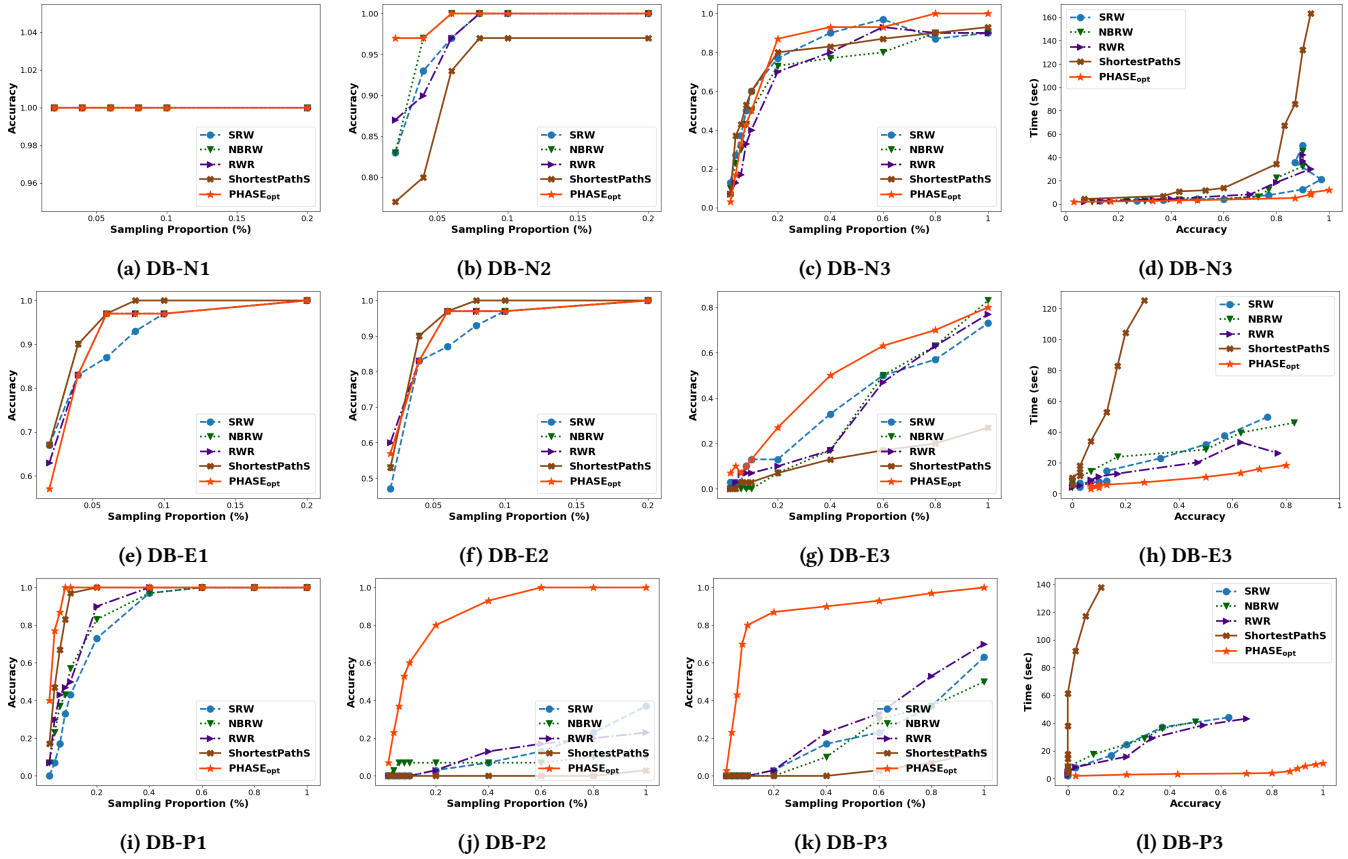


Figure 7: Comparison of the top five sampling methods for accuracy and time (d, h, l) efficiency across three node (a, b, c), three edge (e, f, g), and three path hypotheses (i, j, k) for the DBLP dataset.

path hypotheses, which may also be attributed to the betweenness centrality of those paths in \mathcal{G} .

Figure 5 shows how path length affects accuracy using the DBLP dataset. PHASE_{opt} enables faster convergence of accuracy with longer path lengths, outperforming other samplers.

4.6 Scalability

In Table 4, samplers’ execution time increases as the dataset becomes larger. Among them, *RNS* generally exhibits the shortest execution time as it uniformly samples nodes randomly. The performance of PHASE_{opt} varies across datasets. For the Yelp dataset, it ranks among the highest, particularly for the path hypothesis. This can be attributed to the limited node types in Yelp, resulting in longer extraction times for condensed relevant paths from \mathcal{S} . For the DBLP dataset, PHASE_{opt} ranks among the lowest five. However, instead of considering execution time alone, we should consider both execution time and accuracy performance to evaluate a sampler’s efficiency and effectiveness.

For the top five samplers ranked by their accuracy performance, we plot their accuracy versus execution time in subfigures d, h, and l of Figures 7 and 8. Due to space limitations, only the third hypothesis, which consists of the least number of relevant nodes, edges, or paths in the input graph, of each type is included. First of

all, we observe that the curve of PHASE_{opt} is always at the bottom among others. This means that PHASE_{opt} consistently achieves high accuracy in the shortest amount of time across all plots. Additionally, its execution time does not exhibit exponential growth compared to other existing hypothesis-agnostic samplers. This can be attributed to PHASE_{opt}’s hypothesis-awareness, which allows it to efficiently sample relevant nodes, edges, and paths from the input graph to verify the hypothesis.

The impact of path length on accuracy and execution time is illustrated in Figure 6. As the path length increases, PHASE_{opt} consistently achieves the highest accuracy within the shortest execution time.

5 RELATED WORK

There has been a lot of research interest on hypothesis testing [2, 5, 8, 9, 14, 22, 31], proposing sampling techniques on graphs [16–18]. In this section we summarize the most representative works.

Hypothesis Testing on Graphs. Hypotheses on graphs can be categorized by their object of interest [2, 4, 32]. Tang et al. and Ghoshdastidar et al. [6, 7, 28] extend the one-sample problem into two-sample to test whether two groups of random graphs are obtained by the same generative model or with the same graph distribution. In [31], nodes are objects of interest, and one-sample

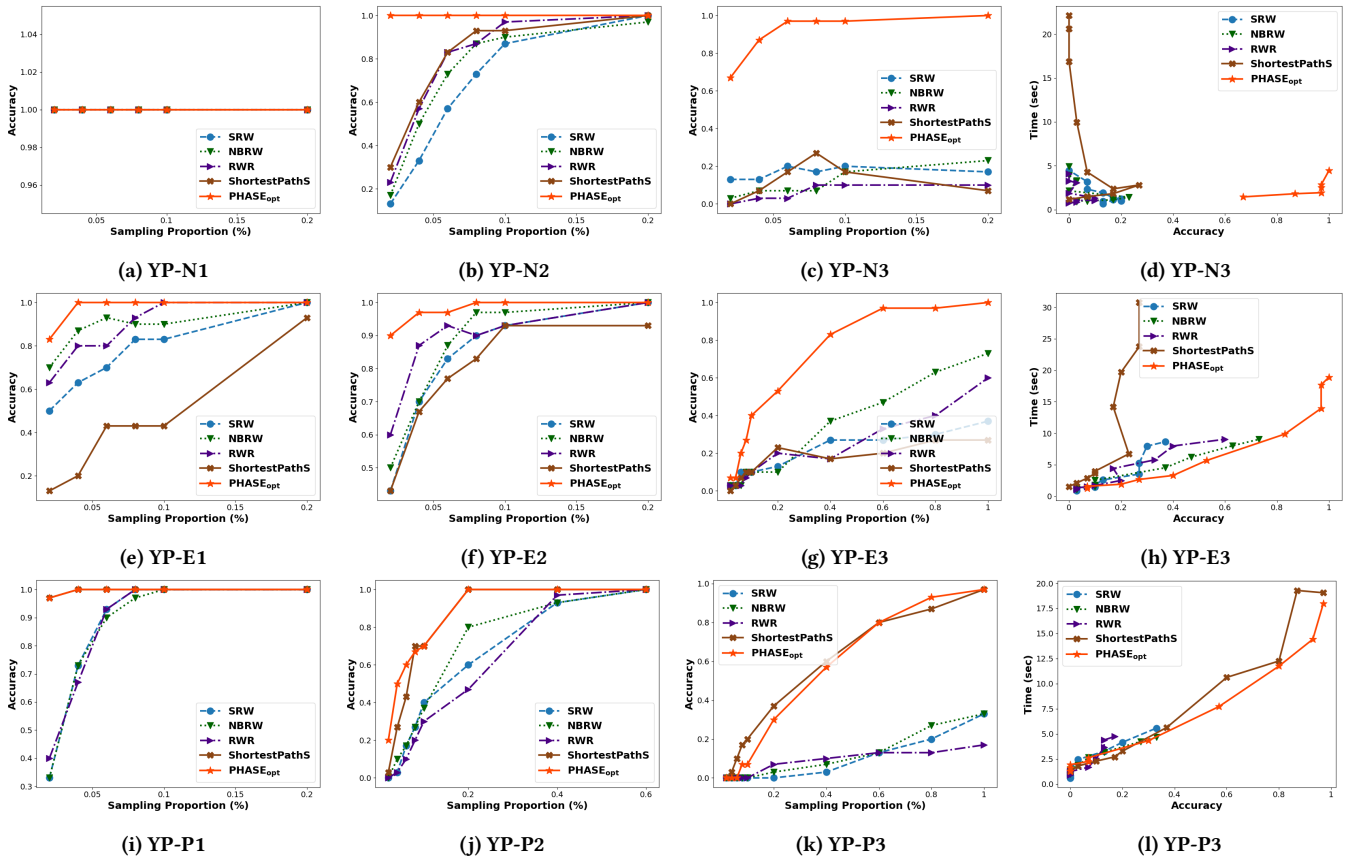


Figure 8: Comparison of the top five sampling methods for accuracy and time (d, h, l) efficiency across three node (a, b, c), three edge (e, f, g), and three path hypotheses (i, j, k) for the Yelp dataset.

hypothesis testing is used to detect conditional dependence between nodes in brain connectivity networks.

Our goal is more related to works when the object of interest is nodes. However, there are two differences between our work and the existing ones. First, we enable more expressive hypotheses, including edge and path hypothesis, on graphs. Second, we leverage graph sampling methods on graph hypothesis testing.

Sampling Methods on Graphs. Most sampling methods are designed to sample a representative subgraph to accurately estimate graph properties [13, 17, 20, 26]. Leskovec and Faloutsos [17] are the first to study this problem in real-world networks [17] by proposing sampling techniques to maintain degree distribution, clustering coefficient and distribution of component sizes. Hübler et al. [13] propose the Metropolis-Hastings sampling method. Later, Maiya and Berger-Wolf [20] propose a community representativeness sample and design a community structure expansion sampler. Many sampling methods are proposed to improve the efficiency and convergence rate of simple random walk [16, 18]. Besides representative sampling, other sampling methods are designed for specific tasks, such as graph compression [3], community detection [20], and graph visualization [23, 30]. However, none of them is designed for hypothesis testing on attributed graphs.

6 CONCLUSION

In this paper, we developed a framework for hypothesis testing on large attributed graphs. Our framework accommodates eleven common hypothesis-agnostic samplers as well as new hypothesis-aware samplers. We proposed dedicated optimizations to speed up sampling while achieving high test significance and accuracy. We demonstrated theoretically and empirically that the convergence rate of our hypothesis-aware sampling.

Our work opens several new directions in the area of hypothesis sampling on graphs. The first direction is to examine additional optimizations that make use of domain-specific information on the input graph. The second direction is to handle more expressive hypotheses and specify two-sample and multiple sample scenarios.

REFERENCES

- [1] Lada A. Adamic, Rajan M. Lukose, Amit R. Puniyani, and Bernardo A. Huberman. 2001. Search in Power-Law Networks. *CoRR* cs.NI/0103016 (2001).
- [2] Ery Arias-Castro and Nicolas Verzelen. 2014. Community detection in dense random networks. (2014).
- [3] Maciej Besta, Simon Weber, Lukas Gianinazzi, Robert Gerstenberger, Andrey Ivanov, Yishai Oltchik, and Torsten Hoefler. 2019. Slim graph: practical lossy graph compression for approximate graph processing, storage, and analytics. In *Proceedings of the International Conference for High Performance Computing, Networking, Storage and Analysis, SC 2019, Denver, Colorado, USA, November 17-19, 2019*. ACM, 35:1–35:25.

- [4] Peter J. Bickel and Purnamrita Sarkar. 2013. Hypothesis Testing for Automated Community Detection in Networks. *CoRR* abs/1311.2694 (2013).
- [5] Darren P Croft, Joah R Madden, Daniel W Franks, and Richard James. 2011. Hypothesis testing in animal social networks. *Trends in ecology & evolution* 26, 10 (2011), 502–507.
- [6] Debarghya Ghoshdastidar, Maurilio Gutzeit, Alexandra Carpentier, and Ulrike von Luxburg. 2017. Two-Sample Tests for Large Random Graphs Using Network Statistics. In *Proceedings of the 30th Conference on Learning Theory, COLT, Amsterdam, The Netherlands, 7-10 July (Proceedings of Machine Learning Research)*, Vol. 65. PMLR, 954–977.
- [7] Debarghya Ghoshdastidar, Maurilio Gutzeit, Alexandra Carpentier, and Ulrike Von Luxburg. 2020. Two-sample hypothesis testing for inhomogeneous random graphs. (2020).
- [8] Debarghya Ghoshdastidar and Ulrike von Luxburg. 2018. Practical Methods for Graph Two-Sample Testing. In *Advances in Neural Information Processing Systems 31: Annual Conference on Neural Information Processing Systems 2018, NeurIPS 2018, December 3-8, 2018, Montréal, Canada*. 3019–3028.
- [9] Connor P. Gibbs, Bailey K. Fosdick, and James D. Wilson. 2022. ECoHeN: A Hypothesis Testing Framework for Extracting Communities from Heterogeneous Networks. *CoRR* abs/2212.10513 (2022).
- [10] Minas Gjoka, Maciej Kurant, Carter T. Butts, and Athina Markopoulou. 2010. Walking in Facebook: A Case Study of Unbiased Sampling of OSNs. In *INFOCOM, 29th IEEE International Conference on Computer Communications, Joint Conference of the IEEE Computer and Communications Societies, 15-19 March, San Diego, CA, USA*. IEEE, 2498–2506.
- [11] Leo A Goodman. 1961. Snowball sampling. *The annals of mathematical statistics* (1961), 148–170.
- [12] F. Maxwell Harper and Joseph A. Konstan. 2016. The MovieLens Datasets: History and Context. *ACM Trans. Interact. Intell. Syst.* 5, 4 (2016), 19:1–19:19.
- [13] Christian Hübler, Hans-Peter Kriegel, Karsten M. Borgwardt, and Zoubin Ghahramani. 2008. Metropolis Algorithms for Representative Subgraph Sampling. In *Proceedings of the 8th IEEE International Conference on Data Mining (ICDM 2008), December 15-19, 2008, Pisa, Italy*. IEEE Computer Society, 283–292.
- [14] David R Hunter, Steven M Goodreau, and Mark S Handcock. 2008. Goodness of fit of social network models. *Journal of the american statistical association* 103, 481 (2008), 248–258.
- [15] Vaishnavi Krishnamurthy, Michalis Faloutsos, Marek Chrobak, Li Lao, Jun-Hong Cui, and Allon G. Percus. 2005. Reducing Large Internet Topologies for Faster Simulations. In *NETWORKING: Networking Technologies, Services, and Protocols; Performance of Computer and Communication Networks; Mobile and Wireless Communication Systems, 4th International IFIP-TC6 Networking Conference, Waterloo, Canada, May 2-6, Proceedings (Lecture Notes in Computer Science)*, Vol. 3462. Springer, 328–341.
- [16] Chul-Ho Lee, Xin Xu, and Do Young Eun. 2012. Beyond random walk and metropolis-hastings samplers: why you should not backtrack for unbiased graph sampling. In *ACM SIGMETRICS/PERFORMANCE Joint International Conference on Measurement and Modeling of Computer Systems, SIGMETRICS, London, United Kingdom, June 11-15*. ACM, 319–330.
- [17] Jure Leskovec and Christos Faloutsos. 2006. Sampling from large graphs. In *Proceedings of the Twelfth ACM SIGKDD International Conference on Knowledge Discovery and Data Mining, Philadelphia, PA, USA, August 20-23*. ACM, 631–636.
- [18] Yongkun Li, Zhiyong Wu, Shuai Lin, Hong Xie, Min Lv, Yinlong Xu, and John C. S. Lui. 2019. Walking with Perception: Efficient Random Walk Sampling via Common Neighbor Awareness. In *35th IEEE International Conference on Data Engineering, ICDE, Macao, China, April 8-11*. IEEE, 962–973.
- [19] László Lovász. 1993. Random walks on graphs. *Combinatorics, Paul erdos is eighty 2*, 1-46 (1993), 4.
- [20] Arun S. Maiya and Tanya Y. Berger-Wolf. 2010. Sampling community structure. In *Proceedings of the 19th International Conference on World Wide Web, WWW, Raleigh, North Carolina, USA, April 26-30*. ACM, 701–710.
- [21] Whitney K Newey and Daniel McFadden. 1994. Large sample estimation and hypothesis testing. *Handbook of econometrics* 4 (1994), 2111–2245.
- [22] Behrooz Omidvar-Tehrani, Sihem Amer-Yahia, and Ria Mae Borromeo. 2019. User group analytics: hypothesis generation and exploratory analysis of user data. *VLDB J.* 28, 2 (2019), 243–266.
- [23] Davood Rafiei and Stephen Curial. 2005. Effectively Visualizing Large Networks Through Sampling. In *16th IEEE Visualization Conference, IEEE Vis 2005, Minneapolis, MN, USA, October 23-28, 2005, Proceedings*. IEEE Computer Society, 375–382.
- [24] Bruno F. Ribeiro and Donald F. Towsley. 2010. Estimating and sampling graphs with multidimensional random walks. In *Proceedings of the 10th ACM SIGCOMM Internet Measurement Conference, IMC, Melbourne, Australia - November 1-3*. ACM, 390–403.
- [25] Michael PH Stumpf, Carsten Wiuf, and Robert M May. 2005. Subnets of scale-free networks are not scale-free: sampling properties of networks. *Proceedings of the National Academy of Sciences* 102, 12 (2005), 4221–4224.
- [26] Daniel Stutzbach, Reza Rejaie, Nick G. Duffield, Subhabrata Sen, and Walter Willinger. 2009. On unbiased sampling for unstructured peer-to-peer networks. *IEEE/ACM Trans. Netw.* 17, 2 (2009), 377–390.
- [27] Jie Tang, Jing Zhang, Limin Yao, Juanzi Li, Li Zhang, and Zhong Su. 2008. Arnet-Miner: extraction and mining of academic social networks. In *Proceedings of the 14th ACM SIGKDD International Conference on Knowledge Discovery and Data Mining, Las Vegas, Nevada, USA, August 24-27*. ACM, 990–998.
- [28] Minh Tang, Avanti Athreya, Daniel L Sussman, Vince Lyzinski, Youngser Park, and Carey E Priebe. 2017. A semiparametric two-sample hypothesis testing problem for random graphs. *Journal of Computational and Graphical Statistics* 26, 2 (2017), 344–354.
- [29] Jaime Waters. 2015. Snowball sampling: A cautionary tale involving a study of older drug users. *International Journal of Social Research Methodology* 18, 4 (2015), 367–380.
- [30] Yanhong Wu, Nan Cao, Daniel Archambault, Qiaomu Shen, Huamin Qu, and Weiwei Cui. 2017. Evaluation of Graph Sampling: A Visualization Perspective. *IEEE Trans. Vis. Comput. Graph.* 23, 1 (2017), 401–410.
- [31] Yin Xia and Lexin Li. 2017. Hypothesis testing of matrix graph model with application to brain connectivity analysis. *Biometrics* 73, 3 (2017), 780–791.
- [32] Yunpeng Zhao, Elizaveta Levina, and Ji Zhu. 2011. Community extraction for social networks. *Proceedings of the National Academy of Sciences* 108, 18 (2011), 7321–7326.